Gastroenterology 2014;146:1060–1069

Gluconeogenic Signals Regulate Iron Homeostasis via Hepcidin in Mice

Chiara Vecchi, Giuliana Montosi,[§] Cinzia Garuti,[§] Elena Corradini, Manuela Sabelli, Susanna Canali, and Antonello Pietrangelo

Center for Hemochromatosis and Metabolic Liver Diseases, Department of Medical and Surgical Sciences, University Hospital of Modena, Modena, Italy

BACKGROUND & AIMS: Hepatic gluconeogenesis provides fuel during starvation, and is abnormally induced in obese individuals or those with diabetes. Common metabolic disorders associated with active gluconeogenesis and insulin resistance (obesity, metabolic syndrome, diabetes, and nonalcoholic fatty liver disease) have been associated with alterations in iron homeostasis that disrupt insulin sensitivity and promote disease progression. We investigated whether gluconeogenic signals directly control Hepcidin, an important regulator of iron homeostasis, in starving mice (a model of persistently activated gluconeogenesis and insulin resistance). **METHODS:** We investigated hepatic regulation of Hepcidin expression in C57BL/6Crl, 129S2/SvPas, BALB/c, and *Creb3l3*−/− null mice. Mice were fed a standard, iron-balanced chow diet or an iron-deficient diet for 9 days before death, or for 7 days before a 24- to 48-hour starvation period; liver and spleen tissues then were collected and analyzed by quantitative reverse-transcription polymerase chain reaction and immunoblot analyses. Serum levels of iron, hemoglobin, Hepcidin, and glucose also were measured. We analyzed human hepatoma (HepG2) cells and mouse primary hepatocytes to study transcriptional control of *Hamp* (the gene that encodes Hepcidin) in response to gluconeogenic stimuli using small interfering RNA, luciferase promoter, and chromatin immunoprecipitation analyses. **RESULTS:** Starvation led to increased transcription of the gene that encodes phosphoenolpyruvate carboxykinase 1 (a protein involved in gluconeogenesis) in livers of mice, increased levels of Hepcidin, and degradation of Ferroportin, compared with nonstarved mice. These changes resulted in hypoferremia and iron retention in liver tissue. Livers of starved mice also had increased levels of *Ppargc1a* mRNA and *Creb3l3* mRNA, which encode a transcriptional co-activator involved in energy metabolism and a liver-specific transcription factor, respectively. Glucagon and a cyclic adenosine monophosphate analog increased promoter activity and transcription of *Hamp* in cultured liver cells; levels of *Hamp* were reduced after administration of small interfering RNAs against *Ppargc1a* and *Creb3l3*. PPARGC1A and CREB3L3 bound the Hamp promoter to activate its transcription in response to a cyclic adenosine monophosphate analog. *Creb3l3*−/− mice did not up-regulate *Hamp* or become hypoferremic during starvation. **CONCLUSIONS:** We identified a link between glucose and iron homeostasis, showing that Hepcidin is a gluconeogenic sensor in mice during starvation. This response is involved in hepatic metabolic adaptation to increased energy demands; it preserves tissue iron for vital activities during food withdrawal, but can cause excessive iron retention and hypoferremia in disorders with persistently activated gluconeogenesis and insulin resistance.

Keywords: Peroxisome Proliferator-Activated Receptor-Gamma Co-activator 1-Alpha (PGC1A); cAMP Response Element-Binding Protein-H (CREBH); Glucagon; Mouse Model.

Adaptation to different states, such as exercise, rest, and starvation or overnutrition, is essential for life. In turn, dysfunction and perturbation of these networks can lead to metabolic imbalances, which if uncorrected induce diseases such as obesity or diabetes. Metabolic adaptation is largely controlled by transcriptional co-regulators and transcription factors responsible, respectively, for sensing metabolic disturbances and fine-tuning the transcriptional response.[1] During starvation, this adaptive response is essential for species survival, and the liver plays a central role in this process as a main site for gluconeogenesis and energy production.[2] At early stages, the liver mobilizes glucose from its glycogen stores; as fasting progresses, it oxidizes fat to provide both energy for gluconeogenesis and substrate for ketogenesis. Generation of sugar from nonsugar carbon substrates (gluconeogenesis) involves several enzyme-catalyzed reactions that take place in both cytosol and mitochondria.

Iron is essential for vital redox activities in the cell, in particular it is required for respiration and energy production in mitochondria (which are also the unique site for heme synthesis and the major site for Fe-S cluster biosynthesis), and likewise is important for mitochondria biogenesis.[3] A number of iron abnormalities, ranging from low serum iron/iron-restricted anemia to hepatic/systemic iron overload, have been reported in human disorders with activated gluconeogenic signaling pathways, including obesity,[4] metabolic syndrome,[5–7] and diabetes.[8,9] Interestingly, iron

[§]Authors share co-senior authorship.

Abbreviations used in this paper: **cAMP, cyclic adenosine monophosphate; ChIP, chromatin immunoprecipitation; CREBBL3/CREBH, cyclic adenosine monophosphate response element binding protein 3–like 3; ER, endoplasmic reticulum; FPN1, ferroportin; HAMP, hepcidin; IL, interleukin; NAFLD, nonalcoholic fatty liver disease; Pck1, phosphoenolpyruvate carboxykinase 1; PPARGC1A, peroxisome proliferator-activated receptor gamma coactivator 1-α; qRT-PCR, quantitative reverse-transcription polymerase chain reaction; siRNA, small interfering RNA.**

© 2014 by the AGA Institute
0016-5085/$36.00
http://dx.doi.org/10.1053/j.gastro.2013.12.016

excess has been associated with worsened insulin sensitivity and disease progression, whereas iron removal has been found to be beneficial.[6,8,10] Based on these premises, we asked whether iron status could be regulated directly by gluconeogenic signals.

Systemic and local iron status are under the control of hepcidin, a defensin-like circulating peptide that degrades the iron exporter ferroportin (FPN1), thereby dictating the extent of iron release or retention in the cell.[11] Hepcidin expression is transcriptionally controlled by a number of factors that deliver the relevant stimulatory or inhibitory signals to the nuclear machinery and turn on or off the hepcidin (*HAMP*) gene. The main stimulatory transcription factors include small mother against decapentaplegic (*SMAD*) proteins, which bind the bone morphogenetic protein responsive element and deliver the "iron signal,"[12,13] STAT-3, mainly involved in the inflammatory signal,[14–16] and cyclic adenosine monophosphate (cAMP) response element binding protein 3–like 3, CREB3L3 (also known as CREBH), more recently found to mediate hepcidin induction by endoplasmic reticulum (ER) stress[17] triggered by a variety of physiological and pathophysiological states.[18–20]

Therefore, we focused on investigating the regulation of hepcidin expression in the liver in response to gluconeogenic stimuli. To this end, we studied mice undergoing prolonged starvation, a classic model of persistently activated gluconeogenesis and insulin resistance.

Materials and Methods

Animal Studies

The starvation experiment was as follows: 8- to 10-week-old male C57BL/6Crl, 129S2/SvPas, BALB/c wild-type mice, and *Creb3l3*-/- null mice (The Jackson Laboratory, Bar Harbor, ME) were allowed free access to water and fed a standard, iron-balanced chow diet in pellets (2018S Teklad Global 18% Protein Rodent Diet; Harlan Laboratories, (San Pietro Al Natisone, UD, Italy); iron content, 225 mg/kg) or starved up to 48 hours starting at the beginning of the light cycle.

Iron-deficient diet experiments were as follows: 8-week-old male C57BL/6Crl wild-type mice were fed an iron-deficient diet (ssniff EF R/M Iron Deficient; Charles River, Calco, LC, Italy; iron content, $<$10 mg/kg) for 9 days before death, or for 6 days before the 24- to 48-hour starvation period.

All animals received humane care according to the criteria outlined by the Federation of European Laboratory Animal Science Associations. The study was approved by the Ethics Committee for Animal Studies at the University of Modena and Reggio Emilia.

Blood Measurements and Tissue Iron Content

Serum iron, serum ferritin (Tina-quant Ferritin kit; Roche Diagnostics, Milan, Italy), hemoglobin, and glucose were determined using an automated COBAS C501 counter (Roche, Milan, Italy) at the clinical-chemical laboratory of the University Hospital of Modena. Serum hepcidin was determined using an enzyme-linked immunosorbent assay kit (USCN Life Science, Hubei, China) according to the manufacturer's instructions, as previously reported.[9] Serum ketone bodies were analyzed using a β-Hydroxybutyrate Assay Kit (Sigma-Aldrich, Milan, Italy) following the manufacturer's instructions.

Liver and spleen tissue specimens were analyzed for non-heme iron content as previously reported.[21]

Real-Time Quantitative Reverse-Transcription Polymerase Chain Reaction and Semiquantitative Reverse-Transcription Polymerase Chain Reaction

Total cellular RNA was obtained by incubating cells in iScript quantitative reverse-transcription polymerase chain reaction (qRT-PCR) Sample Preparation Reagent (Bio-Rad, Milan, Italy) according to the manufacturer's instructions. Total hepatic RNA was extracted as described.[17] Complementary DNA was generated by reverse transcription of 2 μL of iScript buffer (for cultured cells) or 1 μg (for liver) with 200 U ImProm-II Reverse Transcriptase (Promega, Milan, Italy) following the manufacturer's instructions. Expression of mRNA was analyzed using SsoFast EvaGreen Supermix (Bio-Rad). Primer sequences are listed in Supplementary Table 1. Cycling conditions were as follows: 30 seconds at 98°C, followed by 40 cycles of 2 seconds at 98°C and 10 seconds at 60°C. After 40 amplification cycles, threshold cycle values were calculated automatically using the default settings of the CFX Manager software (version 2.0; Bio-Rad), and femtograms of starting complementary DNA were calculated from a standard curve covering a range of 5 orders of magnitude. At the end of the PCR run, melting curves of the amplified products were obtained and used to determine the specificity of the amplification reaction. In each experiment, the change of specific mRNA expression was reported as the fold increase as compared with that of control cells or mice. Normalization of qRT-PCR data was based on *RPL19* housekeeping mRNA expression after validation using the target stability value obtained from the CFX Manager software (version 2.0; Bio-Rad).[22] X-box binding protein 1 (*Xbp1*) splicing was analyzed as described by Vecchi et al.[17] Primer sequences are listed in Supplementary Table 1. The *Hamp* oligos detects total *Hamp* mRNA (*Hamp1* and *Hamp2* mRNA).

Western Blot Analyses

For the FPN1 assay, mouse liver specimens were homogenized in lysis buffer (150 mmol/L NaCl, 10 mmol/L Tris, pH = 8, 1 mmol/L EDTA, 0.5% Triton X-100) containing 1:100 protease inhibitor cocktail (Sigma-Aldrich). After centrifugation at 13,000 $\times$ g at 4°C for 15 minutes, the supernatant was collected and the protein concentration was assayed by the Bradford method. A total of 60 μg of liver extracts were loaded without boiling on 10% acrylamide gels with Laemmli sample buffer, and run in sodium dodecyl sulfate–polyacrylamide gel electrophoresis buffer.

Membranes were probed with specific antibodies: rabbit anti-FPN1 (1:1000; Alpha Diagnostic, Inc, San Antonio, TX), as previously reported,[23] and mouse anti-tubulin (1:3000; Sigma-Aldrich), followed by appropriate horseradish-peroxidase–conjugated secondary antibodies. Western blot analysis was performed by Western Lightning Ultra substrate (PerkinElmer,

Waltham, MA) according to the manufacturer's instructions. Chemiluminescence was detected and quantified using the Molecular Imager ChemiDoc XRS+ with Image Lab Software (Bio-Rad).

Cell Cultures and Primary Hepatocyte Isolation

Human hepatoma HepG2 cells were cultured in Modified Eagle's Medium (MEM) (containing 1 g/L glucose), supplemented with 1 mmol/L glutamine, 100 U/mL penicillin, 100 μg/mL streptomycin, and 10% heat-inactivated fetal bovine serum, in a 5% CO_2 atmosphere at 37°C.

Mouse primary hepatocytes from 8- to 10-week-old male C57BL/6Crl mice were isolated as previously described.[21]

HepG2 cells and mouse primary hepatocytes were incubated for 8 hours in the presence of 1 mmol/L of 8Br cAMP (Sigma-Aldrich) or for 6 hours in the presence of 100 nmol/L of glucagon (Sigma-Aldrich), both in 2% fetal bovine serum culture medium.

Plasmids, Small Interfering RNAs, Transfection, and Luciferase Assay

Hepcidin promoter construct, plasmid encoding Flag-tagged CREB3L3-N (the active form of the factor), *CREB3L3* small interfering RNA (siRNA) transfection, and luciferase analysis have been reported elsewhere.[17] Plasmid encoding peroxisome proliferator-activated receptor gamma coactivator 1-α (PPARGC1A) was kindly provided by Dr Chang Liu (Nanjing, China). *PPARGC1A* siRNA were obtained from Invitrogen (Life Technologies Italia, Monza, Italy) (PPARGC1AHSS116799).

Chromatin Immunoprecipitation

Chromatin immunoprecipitation (ChIP) was described elsewhere[17] with the following modifications. Briefly, HepG2 cells were transfected using X-tremeGENE transfection reagent (Roche Applied Science, Milan, Italy) with plasmid encoding Flag-tagged CREB3L3-N. Forty-eight hours after transfection, cells were treated with 1 mmol/L 8Br cAMP for 8 hours and fixed for formaldehyde cross-linking and ChIP. Protein–DNA complexes were immunoprecipitated overnight using the following antibodies: anti-Flag (Sigma-Aldrich), anti-PPARGC1A (anti-PGC1A; Santa Cruz Biotechnology, Dallas, TX), or anti-green fluorescent protein (GFP) (Abcam, Cambridge, UK) as negative control.

Statistical Analyses

All data were controlled for normal distribution (Kolmogorov–Smirnov and Shapiro–Wilk tests). When comparing a variable in 2 groups, a paired *t* test or the Wilcoxon–Mann–Whitney test was used, depending on the presence or absence of normal data distribution and/or small sample size. When making multiple statistical comparisons on a single data set, for normally distributed data a 1-way analysis of variance with the Tukey or Dunnett post hoc tests, depending on the presence or absence of homoscedasticity, was used. For skewed data, the Kruskal–Wallis test was used. In all statistical analyses, a *P* value less than .05 was considered significant. Data presented in Figures are mean ± SEM. All analyses were conducted using Prism 5 for mac OS X version 5.0a software (GraphPad Software, Inc, La Jolla, CA).

Results

In starving mice, phosphoenolpyruvate carboxykinase 1 (*Pck1*) mRNA, known to be readily responsive to gluconeogenic stimuli, rapidly increased at 2 hours (Figure 1*A*), whereas *Hamp* mRNA increased at 5 hours, in concomitance with a marked serum glucose decrease, and remained increased for up to 48 hours (Figure 1*B*). In addition, serum hepcidin showed a sharp increase at 5 hours, although slightly decreased at later time points (Figure 1*C*). *Hamp* induction led to a decrease of serum iron, and a progressive increase of serum ferritin and iron content in the spleen and the liver (Table 1). In agreement with the hepcidin model of iron regulation, which implies a post-translational down-regulation of ferroportin protein by hepcidin, hepatic *Fpn1* mRNA was unchanged (Figure 1*D*) whereas FPN1 protein was degraded in a time-dependent manner starting at 5 hours' starvation (Figure 1*E* and *F*). A visible ferroportin down-regulation in the spleen was not detected (data not shown). As discussed earlier, the main stimuli for hepcidin transcription in vivo are increased serum and hepatic iron,[24] and cytokines produced during inflammation and infection, particularly interleukin 6 (IL6),[25] IL22,[26] tumor necrosis factor-α,[27] and ER stress.[17] In mice undergoing prolonged starvation, we were unable to detect up-regulation of cytokines such as IL6 and tumor necrosis factor-α, whereas IL22 actually was depressed by food withdrawal (Supplementary Figure 1*A–C*). IL1β was induced by short-term fasting but returned to normal at 48 hours (Supplementary Figure 1*D*), when hepcidin mRNA expression was still increased markedly. Similar negative results were found when analyzing inflammation marker C-reactive protein (*Crp*) mRNA (Supplementary Figure 1*E*) and ER stress markers (namely, *Xbp1* mRNA splicing; Supplementary Figure 1*F*). To address whether hypoferremia in starving mice was caused by lower iron intake associated with food deprivation, we studied mice premaintained on an iron-deprived diet for 1 week. After the iron-deficient diet, this group of mice showed normal serum iron levels (Figure 2*A*), but almost halved spleen iron stores compared with fed mice maintained on an iron-balanced diet (Figure 2*B*), suggesting a marked iron redistribution from the storage site toward the bloodstream to sustain red cell production and maintain normal hemoglobin levels (Figure 2*C*). However, even under this circumstance, starvation led to a progressive decrease of serum iron (Figure 2*A*). Moreover, hepcidin mRNA expression, although depressed in control mice (iron-deficient group) likely because of the latent iron-deficiency state and active marrow activity, still dramatically was induced by starvation (Figure 2*D*). Activation of hepcidin and perturbation of iron homeostasis during starvation-induced gluconeogenesis also was found in other tested mouse strains, such as BALB/c (Supplementary Figure 2*A–C*) or 129S2 (Supplemental Figure 2*D–F*). Overall, these data suggested that, in starving mice, stimuli that are independent of inflammation and/or stress may be responsible for hepcidin induction.

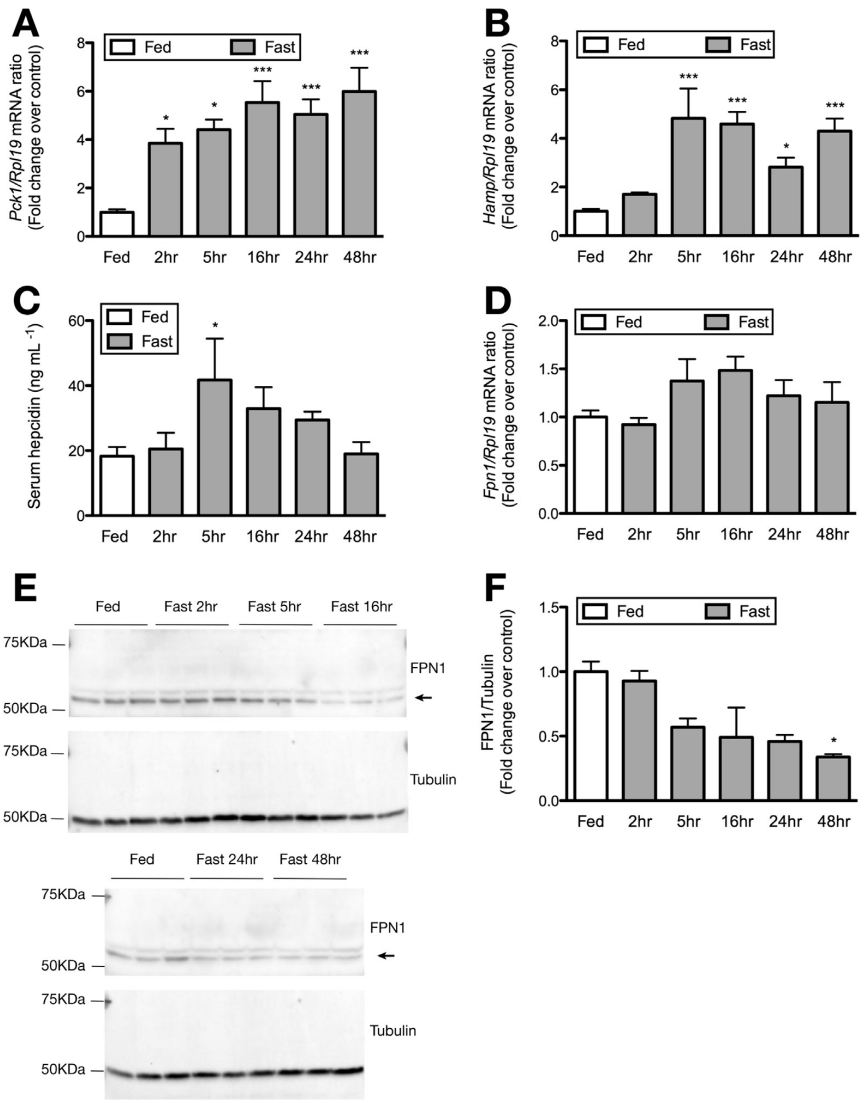

Figure 1. In vivo time course of hepcidin and ferroportin expression in mice during starvation. (*A*) Real-time qRT-PCR analysis of *Pck1* mRNA and (*B*) *Hamp* mRNA expression relative to housekeeping *Rpl19* mRNA in C57BL/6 mice fed a standard diet (*white bar*) or starved for the indicated time periods (*gray bars*). (*C*) Enzyme-linked immunosorbent assay quantification of serum hepcidin levels. (*D*) *Fpn1* mRNA expression relative to housekeeping *Rpl19* mRNA. (*E*) Western blot analysis of FPN1 protein expression in the liver, with tubulin as loading control. The *arrow* indicates the specific FPN1 band, whereas the nonspecific upper band is owing to the secondary antibody. (*F*) Densitometric quantification of FPN1 protein expression relative to tubulin. Results are mean ± SEM of 6–8 mice per group. In Western blot analysis, 3 representative mice per group are shown. For mRNA expression analysis, mean control values for the fed mice group are set to 1. *P* values are reported for comparisons between fed mice and mice fasted at each time point. $^{*}P < .05$, $^{***}P < .001$.

To identify the molecular basis for this novel hepcidin regulatory mechanism, we used an in vitro approach.

The hepatic expression of genes encoding gluconeogenic enzymes, such as *PCK1*, is regulated by a network of transcription factors and cofactors, including CREB proteins[28,29] and PPARGC1A.[30] We recently found that a member of the CREB family, CREBH, is engaged constitutively on the hepcidin promoter and readily transactivates it during ER stress.[17] Both *Ppargc1a* and *Creb3l3* mRNA are induced by hepatic gluconeogenesis in vivo during starvation (Figure 3*A* and *B*). We hypothesized that CREBH is a target for PPARGC1A coactivation during hepcidin induction by active gluconeogenesis. In line with this hypothesis, *PPARGC1A* silencing in HepG2 cells led to a 60% decrease of hepcidin mRNA expression, similar to the effect obtained by *CREB3L3* knockdown (Figure 3*C*).

Gluconeogenesis induced by food deprivation involves cAMP as the main intracellular second messenger in response to hormonal stimuli.[31,32] HepG2 cells exposed to 8Br cAMP, a cAMP analog, showed a significant increase of both *PCK1* and *HAMP* mRNA in a time-dependent manner (Figure 4*A*). A similar trend of hepcidin activation also was found in primary hepatocytes exposed to either glucagon or 8Br cAMP. Both treatments induced *Pck1* and *Hamp* mRNA expression in cultured hepatocytes, although *Hamp* response was significantly but appreciably lower than in HepG2 cells (Figure 4*B*). Hepcidin stimulation by 8Br cAMP in HepG2 cells transfected with siRNA for either

Table 1. In Vivo Effects of Starvation on Biochemical Parameters in Mice

	Fed	2-h Fast	5-h Fast	16-h Fast	24-h Fast	48-h Fast
Serum glucose, *mg/dL*	249.7 ± 36.83	276.4 ± 29.31	188.0 ± 9.09[a]	193.2 ± 13.61[a]	146.7 ± 39.11[b]	180.7 ± 38.53[b]
Serum iron, *μg/dL*	136.3 ± 3.33	143.6 ± 2.85	138.0 ± 8.12	84.00 ± 2.96[b]	86.62 ± 3.06[b]	87.08 ± 4.41[b]
Serum ferritin, *ng/mL*	204.6 ± 8.78	190.0 ± 25.61	193.5 ± 10.78	286.5 ± 32.53	240.0 ± 12.58	277.0 ± 13.58[a]
Spleen iron, *μg/g dry weight*	776.1 ± 29.31	837.5 ± 64.33	706.7 ± 27.62	905.2 ± 13.66	852.0 ± 56.25	1418 ± 58.28[b]
Liver iron, *μg/g dry weight*	224.3 ± 7.39	226.4 ± 9.42	214.9 ± 11.12	231.3 ± 19.73	262.8 ± 16.56	367.1 ± 26.99[b]

NOTE. Serum glucose, serum iron, serum ferritin, and tissue iron levels were analyzed in spleen and liver tissue of wild-type starving and nonstarving mice. Results are mean ± SEM of 6–8 mice per group. *P* values are reported for comparisons between fed and each time-point fasted mice.
[a]$P < .01$.
[b]$P < .001$.

PPARGC1A or *CREB3L3* was appreciably lower as compared with 8Br cAMP-treated control cells (Figure 4*C*). A similar effect was documented when we tested the response of *Hamp* promoter to 8Br cAMP in the presence of *PPARGC1A* or *CREB3L3* siRNAs (Figure 4*D*). To prove that *PPARGC1A* cooperates with CREBH to turn on hepcidin in response to gluconeogenesis, we assessed if the coactivator PPARGC1A/CREBH transduces and binds the hepcidin promoter in response to gluconeogenic stimuli. Overexpression of PPARGC1A in HepG2 cells led to a significant transactivation of the *Hamp* promoter, indicating that the transcription factor is involved in hepcidin promoter regulation (Figure 4*E*). In a previous study we showed that CREBH constitutively occupies the HAMP promoter and transactivates it in response to ER stress.[17] Here, the ChIP assay showed that, in addition to the known constitutive hepcidin promoter occupancy by CREBH (Figure 4*F*, αFlag, control cells), PPARGC1A also constitutively binds to the same region (Figure 4*F*, αPGC1A, control cells). In agreement with the studies reported earlier, after exposure of HepG2 cells to 8Br cAMP, more CREBH was stabilized on the HAMP promoter in the presence of stable PPARGC1A binding (Figure 4*F*, 8Br cAMP-treated cells).

In *Creb3l3* null mice, in agreement with the in vitro studies, starvation correctly induced *Pck1* mRNA (Figure 5*A*), but was unable to activate hepcidin mRNA (Figure 5*B*), modify serum hepcidin levels (Figure 5*C*), or cause hypoferremia (Figure 5*D*). Of note, *Ppargc1a* mRNA was still induced by starvation (Figure 5*E*), but it apparently was unable to stimulate hepcidin expression in the absence of CREBH. These data support a role for CREBH in hepcidin activation by gluconeogenic stimuli in the liver. Interestingly, serum glucose levels were significantly lower in starving

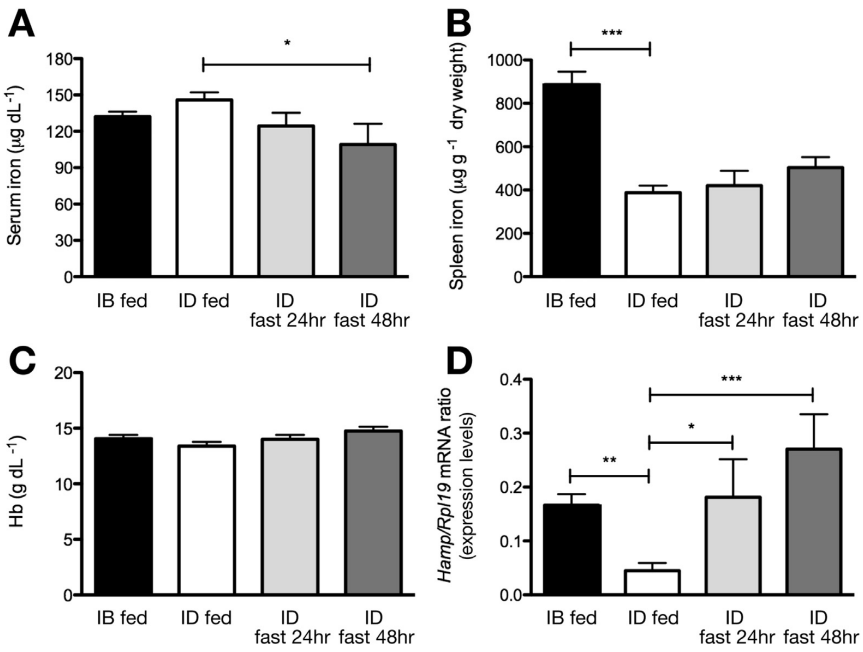

Figure 2. Fasting induces hepcidin gene expression also in mice premaintained on an iron-deficient diet. Eight- to 10-week-old male C57BL/6Crl mice were fed an iron-balanced diet or an iron-deficient diet for 9 days before death (IB and ID, respectively), or for 6 days before the 24- to 48-hour starvation period (ID fast 24-hr and 48 hr). (*A*) Serum iron quantification, (*B*) spleen iron content, (*C*) hemoglobin (Hb) levels, and (*D*) *Hamp* mRNA expression relative to housekeeping *Rpl19* mRNA expression. Results are expressed as the mean ± SEM of 5–6 mice per group. *P* values are reported for comparisons between the indicated groups. $*P < .05$, $**P < .01$, $***P < .001$.

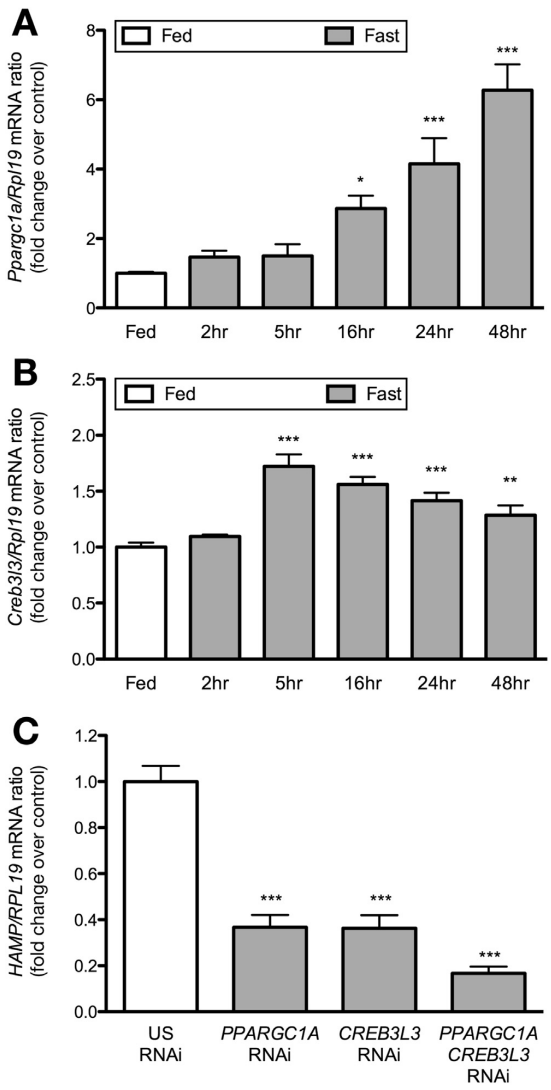

Figure 3. *Ppargc1a* and *Creb3l3* are induced by starvation and are involved in hepcidin expression. (*A*) Real-time qRT-PCR analysis of *Ppargc1a* mRNA and (*B*) *Creb3l3* mRNA expression in liver of C57BL/6 mice fed an iron-standard diet (*white bar*) and starved for the indicated time points (*gray bars*). (*C*) Basal expression of *HAMP* mRNA in HepG2 cells transfected with siRNAs against *PPARGC1A*, *CREB3L3*, or both. Results are mean ± SEM of 6–8 mice per group or 3–4 independent experiments each repeated in triplicate. Mean control values for the fed mice group for in vivo experiments or unspecific (US) RNA interference (RNAi) for in vitro experiments are set to 1 and are normalized relative to housekeeping *Rpl19* mRNA. *P* values are reported for comparisons between control and treated cells, or between indicated groups. $^{*}P < .05$, $^{**}P < .01$, $^{***}P < .001$.

Creb3l3 null mice as compared with starving wild-type mice (Table 2). Seemingly, the increase of serum ketone bodies during starvation was more pronounced in the *Creb3l3* null mice (4.7- to 5.6-fold) as compared with control mice (3.1- to 3.5-fold) (Table 2).

Discussion

Hepcidin is constitutively produced by the liver to maintain plasma iron levels within a narrow physiologic range. To do so it senses a variety of physiologic and pathophysiologic stimuli that tend to alter blood iron levels, and responds by inhibiting ferroportin, the main iron-exporter in mammals.[33] In this study we showed that hepcidin is regulated transcriptionally also by gluconeogenic signals through PPARGC1A/CREBH. Induction of this regulatory pathway in a classic model of insulin resistance/activated gluconeogenesis, ie, starvation, leads to tissue iron retention and circulatory iron deficiency. Hypoferremia is clearly secondary to increased tissue iron retention after hepcidin induction and not to reduced food iron intake because it still is preserved in mice premaintained on an iron-deprived diet (Figure 2). Activation of hepcidin and perturbation of iron homeostasis during starvation-induced gluconeogenesis seem to represent a general defensive response in rodents because it was found in other tested mouse strains. However, differences in terms of the time course of hepcidin induction and the extent of iron status modifications were detected clearly among various starving mice strains. This could be explained by the fact that both the gluconeogenic response/gluconeogenic gene expression and iron status/iron gene expression may vary appreciably among mouse strains, as also documented by the significantly higher expression of the *Pck1* gene in C57BL/6 mice (an optimal mouse model for studying gluconeogenesis/insulin resistance[34,35] and the model that most closely parallels the gluconeogenic response to starvation seen in human beings) as compared with 129S2, BALB/c, and *Creb3l3 null* mice (which actually display a mixed genetic background of 129S1, 129X1, C57BL/6, FVB/N). A close look at the time course induction of *Pck1*/*Hamp* (Figure 1*A* and *B*) and *Ppargc1a*/*Creb3l3* RNAs (Figure 3*A* and *B*) suggests that the initial 5-hour burst of *Hamp* transcription largely depends on increased *Creb3l3* expression. Later, the increase in *Ppargc1A* expression likely sustains hepcidin transcription by enhancing and further stabilizing CREBH binding on the *Hamp* promoter (Figure 4*F*, ChIP study). We were able to reproduce the effect of starvation in vitro, in a hepatoma cell line and cultured primary hepatocytes, using different gluconeogenic stimuli (Figure 4). However, the *Hamp* gene response to gluconeogenic signals in primary hepatocytes was lower than in hepatoma cells. This may depend on the fact that in primary hepatocytes the gluconeogenic signals may be attenuated, as indicated by the lower *Pck1* induction in primary hepatocytes exposed to 8Br cAMP as compared with HepG2 cells (Figure 4*B* vs *A*), and/or that additional factors essential for the hepcidin transcriptional machinery are lost in primary hepatocytes after the disruption of liver architecture/microenvironment.

The newly identified regulatory pathway links glucose and iron metabolism in the liver and identifies hepcidin, the iron hormone, as a gluconeogenic sensor.

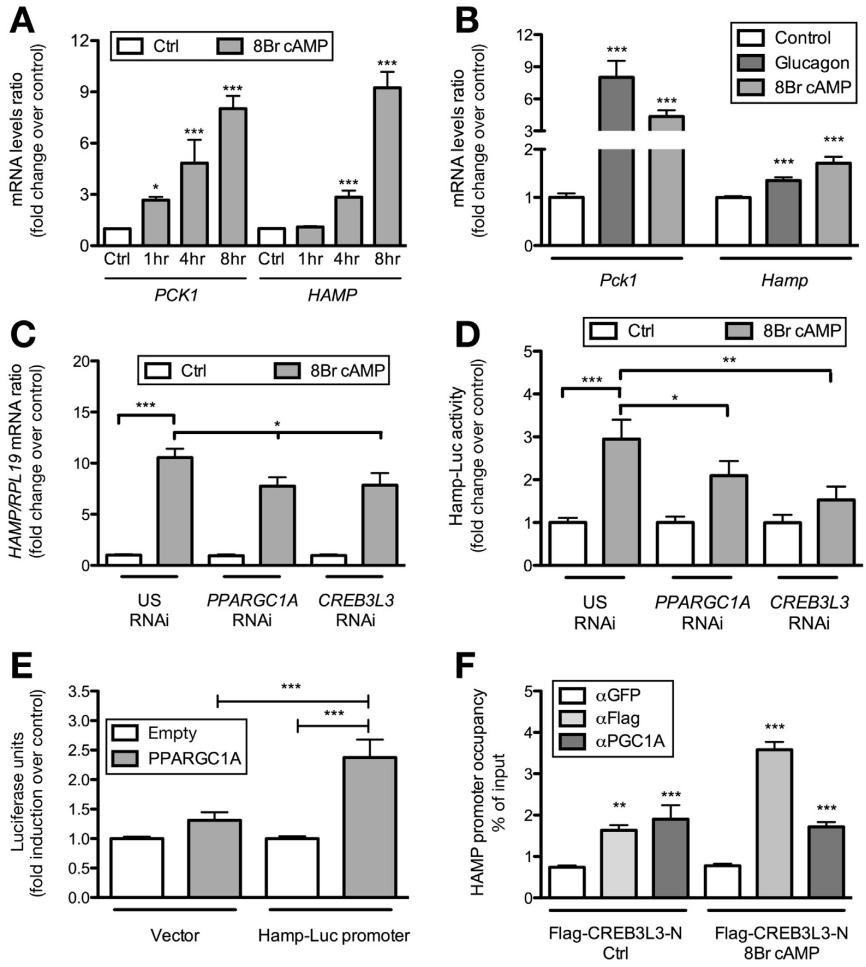

Figure 4. Hepcidin is induced by gluconeogenic signals through PPARGC1A/CREBH. (*A*) HepG2 cells were cultured in the presence of a cAMP analog (8Br cAMP) and analyzed at different time points for *PCK1* and *HAMP* mRNA expression by real-time qRT-PCR. (*B*) *Pck1* and *Hamp* mRNA expression in primary mouse hepatocytes isolated from C57BL/6 mice and exposed to glucagon or 8Br cAMP. (*C*) *HAMP* mRNA expression and (*D*) *Hamp*-promoter luciferase activity in HepG2 cells after silencing of *PPARGC1A* and *CREB3L3*. (*E*) *Hamp*-promoter luciferase activity in HepG2 cells transfected with control plasmid (empty) or construct encoding PPARGC1A protein. (*F*) ChIP assay of HepG2 cells transfected with Flag-tagged CREB3L3-N vector and exposed to 8Br cAMP. CREBH (αFlag) and PPARGC1A (αPGC1A) occupancy of CREBH site on hepcidin endogenous promoter was evaluated by real-time qRT-PCR and expressed as a percentage of the input signal. αGFP (green fluorescent protein) antibody is used as control, unrelated antibody. Results are mean ± SEM of 3–4 independent experiments, each repeated in triplicate. For mRNA and luciferase analysis, mean control values are set to 1. ChIP data are mean ± SEM representative of 2 separate experiments. *P* values are reported for comparisons (*A* and *B*) between control and treated cells, (*C–E*) between indicated groups, or between αGFP and specific antibodies. $^{*}P < .05$, $^{**}P < .01$, $^{***}P < .001$.

PPARGC1A is a transcriptional coactivator that regulates the genes involved in energy metabolism. During starvation, PPARGC1A readily is activated to turn on the gluconeogenic machinery, but also to stimulate mitochondrial biogenesis and respiration,[36] which are essential to support the increased energy demands. Interestingly, in osteoclasts, mitochondrial biogenesis involves CREB/PPARGC1A proteins, but requires iron uptake and supply to mitochondrial respiratory proteins.[37] Here, we found that PPARGC1A constitutively occupies the hepcidin promoter and, in response to gluconeogenic stimuli, stabilizes CREBH binding and transactivates HAMP promoter. CREBH is an ER stress–associated liver-specific transcription factor originally involved in the induction of acute-phase response genes (such as serum amyloid protein and C-reactive protein[38]), and subsequently has been found to activate the transcription of *HAMP*.[17] Based on recent publications and this report, CREBH now emerges as a key metabolic regulator in the liver: it is activated by fatty acids and PPARα,[39,40] and regulates the expression of genes involved in hepatic lipogenesis, fatty acid

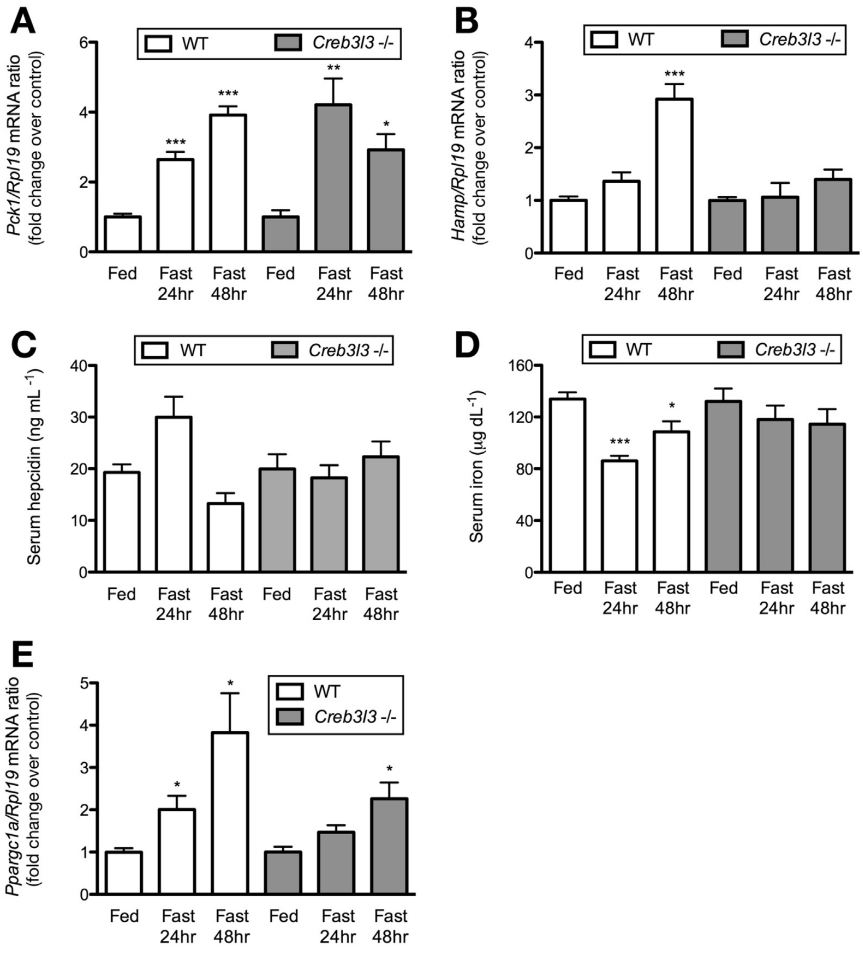

Figure 5. Starvation fails to induce hepcidin gene expression in *Creb3l3*-/- mice. Eight- to 10-week-old wild type (WT) or *Creb3l3*-/- male mice were starved for 24 or 48 hours before death. (*A*) *Pck1* mRNA and (*B*) *Hamp* mRNA expression were assessed by real-time qRT-PCR. (*C*) Enzyme-linked immunosorbent assay quantification of serum hepcidin levels and (*D*) serum iron levels. (*E*) *Ppargc1a* mRNA expression in starved mice. Results are mean ± SEM of 6–8 mice per group. (*A*, *B*, and *E*) Mean control values for the fed mice group are set to 1 and are normalized relative to housekeeping *Rpl19* mRNA. *P* values are reported for comparisons between fed and 24- or 48-hour fasted mice, within each genotype. $^{*}P < .05$, $^{**}P < .01$, $^{***}P < .001$.

oxidation, and lipolysis under metabolic stress.[20] Interestingly, CREBH also has been found to transcriptionally regulate *Pck1* and glucose-6-phosphatase, the critical genes in hepatic gluconeogenic response.[41] Here, we report that CREBH is engaged constitutively on the hepcidin promoter to sense metabolic gluconeogenic stress and modify, accordingly, iron traffic. Of note is that starving *Creb3l3* null mice show reduced glucose and increased ketone body output.

Adaptation to starvation is essential for species survival.[42] Seemingly, defense against pathogens represents a priority in species evolution. The liver, as the main source for hepcidin, seems to play a central role in both processes. During infection, hepcidin limits vital iron that is needed by invading microorganisms, thus contributing to host defense.[25] During prolonged starvation, hepcidin likely preserves tissue iron and helps to maintain energy balance

Table 2. In Vivo Effects of Starvation on Glucose and Ketone Body Status in *Creb3l3* Null Mice

	WT			*Creb3l3* -/-		
	Fed	24-h Fast	48-h Fast	Fed	24-h Fast	48-h Fast
Serum glucose, *mg/dL*	243.7 ± 8.32	146.2 ± 26.91[a]	102.2 ± 12.78[a]	237.6 ± 8.26	95.2 ± 9.24[a]	64.8 ± 9.41[a]
Serum ketone bodies, *mmol/L*	0.54 ± 0.13	1.68 ± 0.10[a]	1.88 ± 0.24[a]	0.39 ± 0.02	1.85 ± 0.17[a]	2.20 ± 0.17[a]

NOTE. Serum glucose and ketone bodies levels were analyzed in WT and *Creb3l3* null mice starved for 24 or 48 hours before sacrifice. Results are mean ± SEM of 6–8 mice per group. *P* value are reported for comparisons between fed and 24- or 48-hour fasted mice, within each genotype.
[a]$P < .001$.

and support gluconeogenesis in the liver (this report). Most likely, this response originally evolved to protect human beings during food withdrawal.

Paradoxically, in human disorders associated with food excess and storage, such as type 2 diabetes, obesity, and the metabolic syndrome, persistently activated gluconeogenesis may result in overstimulation of hepcidin, iron accumulation, and potential damage. Cases of unexplained hepatic iron excess, characterized by high serum ferritin levels with normal or subnormal transferrin saturation, and associated with metabolic abnormalities, originally were reported by Moirand et al,[43] who also introduced the term *iron overload-associated insulin resistance* (recently renamed *dysmetabolic iron overload syndrome*). Hepatocellular and/or mesenchymal iron deposition, usually slight or mild, has been reported since then in nonalcoholic fatty liver disease (NAFLD) and nonalcoholic steatohepatitis.[44] The clinical relevance of iron excess in these disorders, in terms of fibrosis development and cancer risk, is actively debated,[45] but increasing data indicate that iron may sustain disease activity and/or contribute to its progression.[46–49] Interestingly, NAFLD patients with mixed or mesenchymal iron overload (a pattern of iron deposition consistent with a "hepcidin-excess model") seem more likely to develop fibrosis than those with pure parenchymal iron deposits (a pattern of iron deposition consistent with a "hepcidin-deficient model").[47,49] The mechanism of iron deposition in NAFLD/dysmetabolic iron overload syndrome likely is multifactorial: sex, diet, disease activity, genetic background (*HFE* hemochromatosis gene mutations), ethnicity, and (micro)inflammation all may account for the variability of both iron excess and its pattern of distribution. We hypothesize that a fraction of dysmetabolic/NAFLD patients with normal-low transferrin saturation and mixed/mesenchymal hepatic iron deposits may represent a subgroup of patients with prominent insulin resistance and hepcidin induction via the gluconeogenic PPARGC1A/CREBH-driven pathway described here. In these patients, hepcidin, depending on the degree and duration of its induction, may modify iron traffic locally or systemically and lead, respectively, to simple hepatic iron retention with marginal systemic reflections (ie, mesenchymal/mixed hepatic iron accumulation with normal or subnormal transferrin saturation), or substantial tissue iron retention, hypoferremia, and iron-restricted anemia. Further studies are needed to prove that the gluconeogenic signal-driven induction of hepcidin in starving mice also takes place in other instances of activated gluconeogenesis and insulin resistance, such as diabetes, obesity, or NAFLD. If so, because of the increasingly recognized negative effect of iron excess on the progression of these disorders, the novel regulatory pathway reported here may offer potential new therapeutic targets to prevent or correct iron disturbances in common metabolic disorders.

Supplementary Material

Note: To access the supplementary material accompanying this article, visit the online version of *Gastroenterology* at www.gastrojournal.org, and at http://dx.doi.org/10.1053/j.gastro.2013.12.016.

References

1. Spiegelman BM, Heinrich R. Biological control through regulated transcriptional coactivators. Cell 2004; 119:157–167.
2. Cahill GF Jr. Fuel metabolism in starvation. Annu Rev Nutr 2006;26:1–22.
3. Muhlenhoff U, Lill R. Biogenesis of iron-sulfur proteins in eukaryotes: a novel task of mitochondria that is inherited from bacteria. Biochim Biophys Acta 2000;1459:370–382.
4. **Bekri S, Gual P**, Anty R, et al. Increased adipose tissue expression of hepcidin in severe obesity is independent from diabetes and NASH. Gastroenterology 2006; 131:788–796.
5. Mendler MH, Turlin B, Moirand R, et al. Insulin resistance-associated hepatic iron overload. Gastroenterology 1999;117:1155–1163.
6. Facchini FS, Hua NW, Stoohs RA. Effect of iron depletion in carbohydrate-intolerant patients with clinical evidence of nonalcoholic fatty liver disease. Gastroenterology 2002;122:931–939.
7. Valenti L, Dongiovanni P, Fracanzani AL, et al. Blood-letting ameliorates insulin sensitivity and secretion in parallel to reducing liver iron in carriers of HFE gene mutations: response to Equitani, et al. Diabetes Care 2008;31:e18; author reply e19.
8. Fernandez-Real JM, Penarroja G, Castro A, et al. Blood letting in high-ferritin type 2 diabetes: effects on insulin sensitivity and beta-cell function. Diabetes 2002; 51:1000–1004.
9. Jiang F, Sun ZZ, Tang YT, et al. Hepcidin expression and iron parameters change in type 2 diabetic patients. Diabetes Res Clin Pract 2011;93:43–48.
10. Valenti L, Moscatiello S, Vanni E, et al. Venesection for non-alcoholic fatty liver disease unresponsive to lifestyle counselling–a propensity score-adjusted observational study. QJM 2011;104:141–149.
11. Nemeth E, Tuttle MS, Powelson J, et al. Hepcidin regulates cellular iron efflux by binding to ferroportin and inducing its internalization. Science 2004;306:2090–2093.
12. **Andriopoulos B Jr, Corradini E, Xia Y**, et al. BMP6 is a key endogenous regulator of hepcidin expression and iron metabolism. Nat Genet 2009;41:482–487.
13. **Meynard D, Kautz L**, Darnaud V, et al. Lack of the bone morphogenetic protein BMP6 induces massive iron overload. Nat Genet 2009;41:478–481.
14. Wrighting DM, Andrews NC. Interleukin-6 induces hepcidin expression through STAT3. Blood 2006;108:3204–3209.
15. Verga Falzacappa MV, Vujic Spasic M, Kessler R, et al. STAT3 mediates hepatic hepcidin expression and its inflammatory stimulation. Blood 2007;109:353–358.
16. Pietrangelo A, Dierssen U, Valli L, et al. STAT3 is required for IL-6-gp130-dependent activation of hepcidin in vivo. Gastroenterology 2007;132:294–300.
17. Vecchi C, Montosi G, Zhang K, et al. ER stress controls iron metabolism through induction of hepcidin. Science 2009;325:877–880.
18. Misra J, Chanda D, Kim DK, et al. Curcumin differentially regulates endoplasmic reticulum stress through transcriptional corepressor SMILE (small heterodimer

partner-interacting leucine zipper protein)-mediated inhibition of CREBH (cAMP responsive element-binding protein H). J Biol Chem 2011;286:41972–41984.
19. Shin DY, Chung J, Joe Y, et al. Pretreatment with CO-releasing molecules suppresses hepcidin expression during inflammation and endoplasmic reticulum stress through inhibition of the STAT3 and CREBH pathways. Blood 2012;119:2523–2532.
20. Zhang C, Wang G, Zheng Z, et al. Endoplasmic reticulum-tethered transcription factor cAMP responsive element-binding protein, hepatocyte specific, regulates hepatic lipogenesis, fatty acid oxidation, and lipolysis upon metabolic stress in mice. Hepatology 2012; 55:1070–1082.
21. Corradini E, Schmidt PJ, Meynard D, et al. BMP6 treatment compensates for the molecular defect and ameliorates hemochromatosis in Hfe knockout mice. Gastroenterology 2010;139:1721–1729.
22. Vandesompele J, De Preter K, Pattyn F, et al. Accurate normalization of real-time quantitative RT-PCR data by geometric averaging of multiple internal control genes. Genome Biol 2002;3. RESEARCH0034.
23. McDonald CJ, Ostini L, Wallace DF, et al. Iron loading and oxidative stress in the Atm-/- mouse liver. Am J Physiol Gastrointest Liver Physiol 2011;300:G554–560.
24. Pigeon C, Ilyin G, Courselaud B, et al. A new mouse liver-specific gene, encoding a protein homologous to human antimicrobial peptide hepcidin, is overexpressed during iron overload. J Biol Chem 2001;276:7811–7819.
25. Andrews NC. Anemia of inflammation: the cytokine-hepcidin link. J Clin Invest 2004;113:1251–1253.
26. Armitage AE, Eddowes LA, Gileadi U, et al. Hepcidin regulation by innate immune and infectious stimuli. Blood 2011;118:4129–4139.
27. Nemeth E, Valore EV, Territo M, et al. Hepcidin, a putative mediator of anemia of inflammation, is a type II acute-phase protein. Blood 2003;101:2461–2463.
28. Thiel G, Al Sarraj J, Stefano L. cAMP response element binding protein (CREB) activates transcription via two distinct genetic elements of the human glucose-6-phosphatase gene. BMC Mol Biol 2005;6:2.
29. **Koo SH, Flechner L**, Qi L, et al. The CREB coactivator TORC2 is a key regulator of fasting glucose metabolism. Nature 2005;437:1109–1111.
30. Herzig S, Long F, Jhala US, et al. CREB regulates hepatic gluconeogenesis through the coactivator PGC-1. Nature 2001;413:179–183.
31. Yoon JC, Puigserver P, Chen G, et al. Control of hepatic gluconeogenesis through the transcriptional coactivator PGC-1. Nature 2001;413:131–138.
32. Marshall S. Role of insulin, adipocyte hormones, and nutrient-sensing pathways in regulating fuel metabolism and energy homeostasis: a nutritional perspective of diabetes, obesity. cancer. Sci STKE 2006; 2006:re7.
33. Pietrangelo A. Hepcidin in human iron disorders: therapeutic implications. J Hepatol 2011;54:173–181.
34. Champy MF, Selloum M, Zeitler V, et al. Genetic background determines metabolic phenotypes in the mouse. Mamm Genome 2008;19:318–331.
35. Berglund ED, Li CY, Poffenberger G, et al. Glucose metabolism in vivo in four commonly used inbred mouse strains. Diabetes 2008;57:1790–1799.
36. Scarpulla RC. Nuclear control of respiratory chain expression by nuclear respiratory factors and PGC-1-related coactivator. Ann N Y Acad Sci 2008;1147:321–334.
37. Ishii KA, Fumoto T, Iwai K, et al. Coordination of PGC-1beta and iron uptake in mitochondrial biogenesis and osteoclast activation. Nat Med 2009;15:259–266.
38. Zhang K, Shen X, Wu J, et al. Endoplasmic reticulum stress activates cleavage of CREBH to induce a systemic inflammatory response. Cell 2006;124:587–599.
39. **Danno H, Ishii KA**, Nakagawa Y, et al. The liver-enriched transcription factor CREBH is nutritionally regulated and activated by fatty acids and PPARalpha. Biochem Biophys Res Commun 2010;391:1222–1227.
40. Gentile CL, Wang D, Pfaffenbach KT, et al. Fatty acids regulate CREBh via transcriptional mechanisms that are dependent on proteasome activity and insulin. Mol Cell Biochem 2010;344:99–107.
41. **Lee MW, Chanda D**, Yang J, et al. Regulation of hepatic gluconeogenesis by an ER-bound transcription factor, CREBH. Cell Metab 2010;11:331–339.
42. Cahill GF Jr. Starvation in man. Clin Endocrinol Metab 1976;5:397–415.
43. Moirand R, Mortaji AM, Loreal O, et al. A new syndrome of liver iron overload with normal transferrin saturation. Lancet 1997;349:95–97.
44. Corradini E, Pietrangelo A. Iron and steatohepatitis. J Gastroenterol Hepatol 2012;27(Suppl 2):42–46.
45. Pietrangelo A. Iron in NASH, chronic liver diseases and HCC: how much iron is too much? J Hepatol 2009; 50:249–251.
46. Sorrentino P, D'Angelo S, Ferbo U, et al. Liver iron excess in patients with hepatocellular carcinoma developed on non-alcoholic steato-hepatitis. J Hepatol 2009;50:351–357.
47. Turlin B, Mendler MH, Moirand R, et al. Histologic features of the liver in insulin resistance-associated iron overload. A study of 139 patients. Am J Clin Pathol 2001;116:263–270.
48. Valenti L, Fracanzani AL, Bugianesi E, et al. HFE genotype, parenchymal iron accumulation, and liver fibrosis in patients with nonalcoholic fatty liver disease. Gastroenterology 2010;138:905–912.
49. Nelson JE, Wilson L, Brunt EM, et al. Relationship between the pattern of hepatic iron deposition and histological severity in nonalcoholic fatty liver disease. Hepatology 2011;53:448–457.

Author names in bold designate shared co-first authorship.

Received March 28, 2013. Accepted December 6, 2013.

Reprint requests
Address requests for reprints to: Antonello Pietrangelo, MD, Division of Internal Medicine 2 and Center for Hemochromatosis, Department of Medical and Surgical Sciences, University Hospital of Modena, Via del Pozzo 71, 41100 Modena, Italy. e-mail: antonello.pietrangelo@unimore.it.

Conflicts of interest
The authors disclose no conflicts.

Funding
This work was supported by Telethon grant GGP10233 and PRIN grant 2010REYFZH_005 to AP.

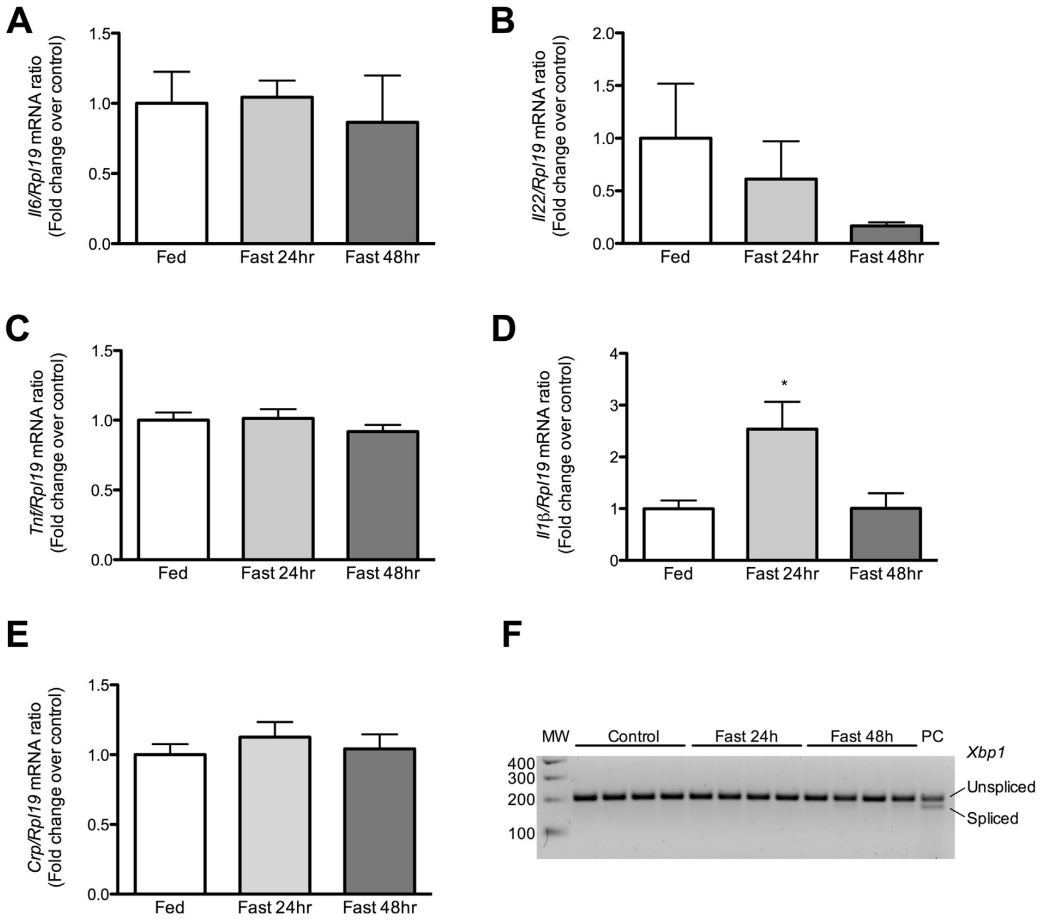

Supplementary Figure 1. Hepatic expression of inflammation or ER stress markers in mice during starvation. Total liver mRNA analysis in liver of C57BL/6 mice fed a standard diet (*white bar*) and starved for the indicated time points (*gray bars*). (*A–D*) Real-time qRT-PCR analysis of cytokine mRNA expression relative to housekeeping *Rpl19* mRNA: (*A*) *Il6*, (*B*) *Il22*, (*C*) *Tnf*, and (*D*) *Il1β*. (*E*) *Crp* mRNA expression, as an inflammatory marker, and (*F*) PCR analysis of *Xbp1* mRNA splicing analysis, as an ER stress marker. Results are mean ± SEM of 6–8 mice per group. For mRNA expression analysis, mean control values for the fed mice group are set to 1. In the *Xbp1* splicing analysis, 3 representative mice per group are shown. MW, molecular weight, PC positive control. *P* values are reported for comparisons between fed mice and fasted mice at each time point. $^*P < .05$.

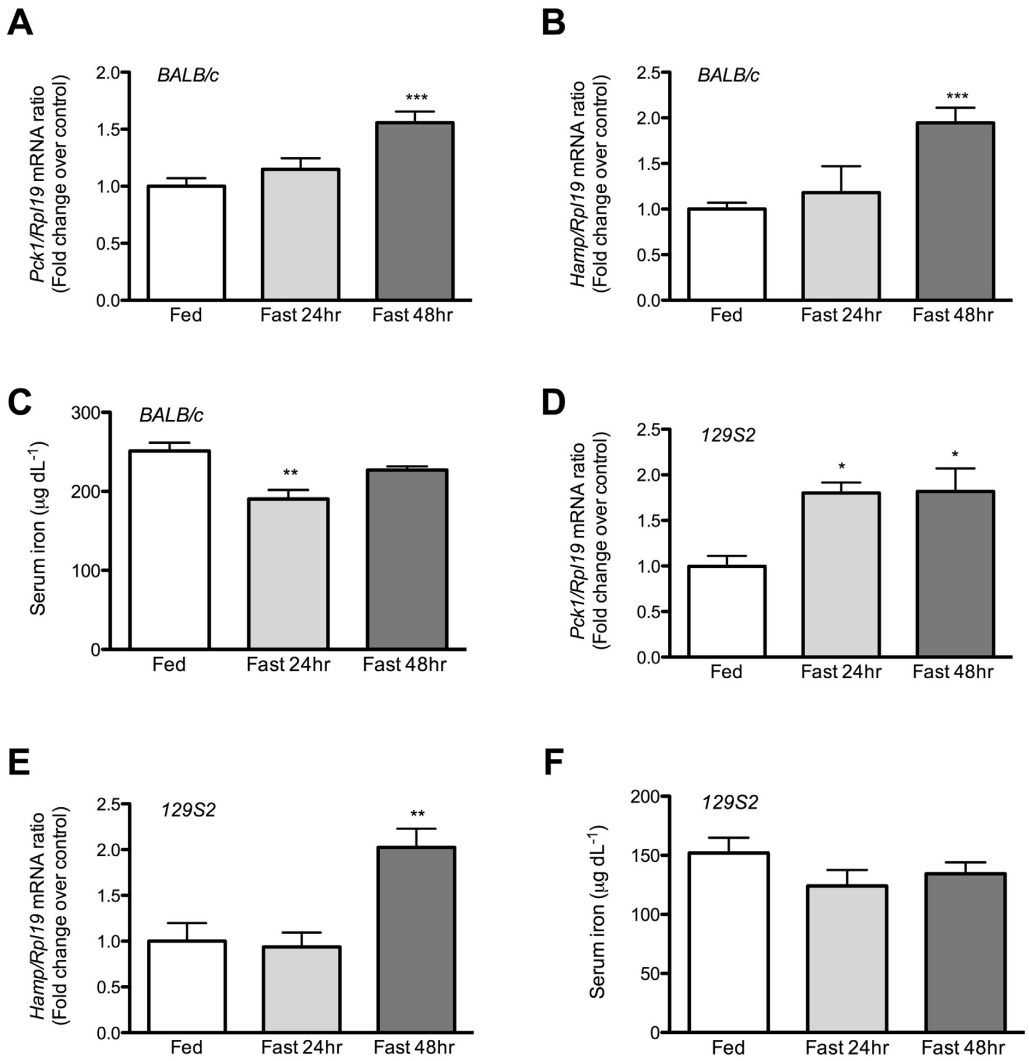

Supplementary Figure 2. Fasting induces hepcidin gene expression and hypoferremia in vivo in BALB/c and 129S2/SvPas (129S2) wild-type mice. Eight- to 10-week-old (*A–C*) BALB/c and (*D–F*) 129S2/SvPas wild-type mice were fasted for 24-48 hours. Real-time qRT-PCR analysis of (*A* and *D*) *Pck1* mRNA, (*B* and *E*) *Hamp* mRNA, and (*C* and *F*) serum iron in fed and fasted mice. Results are expressed as the mean ± SEM of 6–8 mice per group. For mRNA expression analysis in panels *A* and *B* and in *D* and *E*, the mean control values are set to 1 and are normalized relative to housekeeping *Rpl19* mRNA. *P* values are reported for comparisons between control fed mice and fasted mice. $^{*}P < .05$, $^{**}P < .01$, $^{***}P < .001$.

Supplementary Table 1. List of Primers Used for Real-Time qRT-PCR

Accession number	Gene name	Forward	Reverse
Murine oligonucleotides			
NM_032541.1	*Hamp*	5′-GCCTGTCTCCTGCTTCTCCT-3′	5′-GCTCTGTAGTCTGTCTCATCTGTT-3′
NM_011044.2	*Pck1*	5′-AACTGTTGGCTGGCTCTC-3′	5′-GAACCTGGCGTTGAATGC-3′
NM_145365.3	*Creb3l3*	5′-GATACCCTGTACCCGGAGGAG-3′	5′-CGGACAGCAGCAGTTCCTTC-3′
NM_008904.2	*Ppargc1a*	5′-CCGTAAATCTGCGGGATGATG-3′	5′-CAGTTTCGTTCGACCTGCGTAA-3′
NM_031168.1	*Il6*	5′-ATGGATGCTACCAAACTGGAT-3′	5′-TGAAGGACTCTGGCTTTGTCT-3′
NM_008361.3	*Il1b*	5′-CCTTTTCGTGAATGAGCAGACAG-3′	5′-TCTCTTTGAACAGAATGTGCCATG-3′
NM_016971.2	*Il22*	5′-ATGAGTTTTTCCCTTATGGGGAC-3′	5′-GCTGGAAGTTGGACACCTCAA-3′
NM_013693.2	*Tnf*	5′-ATGGCCTCCCTCTCATCAGTT-3′	5′-GGCTACAGGCTTGTCACTCG-3′
NM_007768.4	*Crp*	5′-CTGCACAAGGGCTACACTGT-3′	5′-TCTCCCACCAAAGACTGCTTT-3′
NM_009078.2	*Rpl19*	5′-ATGAGTATGCTCAGGCTACAGA-3′	5′-GCATTGGCGATTTCATTGGTC-3′
NM_016917.2	*Fpn1*	5′-AAGACTCCAACATCCGTGAACTT-3′	5′-GACCCATCCATCTCGGAAAGTG-3′
Human oligonucleotides			
NM_021175.2	*HAMP*	5′-TGTTTTCCCACAACAGACGGG-3′	5′-CGCAGCAGAAAATGCAGATGG-3′
NM_000981.3	*RPL19*	5-′GGGCATAGGTAAGCGGAAGG-3′	5′-TCAGGTACAGGCTGTGATACA-3′
NM_032607.1	*CREB3L3*	5′-CCTCTGTGACCATAGACCTGG-3′	5′-ACGGTGAGATTGCATCGTGG-3′
NM_013261.3	*PPARGC1A*	5′-GCTTTCTGGGTGGACTCAAGT-3′	5′-TCTAGTGTCTCTGTGAGGACTG-3′
NM_002591.3	*PCK1*	5′-GCGGCTGAAGAAGTATGA-3′	5′-GGAACCTGGCATTGAACG-3′